Journal for ImmunoTherapy of Cancer

GD2-targeting CAR-T cells enhanced by transgenic IL-15 expression are an effective and clinically feasible therapy for glioblastoma

Tessa Gargett ,[1,2,3] Lisa M Ebert ,[1,3] Nga T H Truong,[1,2] Paris M Kollis,[1,3] Kristyna Sedivakova,[1,3] Wenbo Yu,[1] Erica C F Yeo,[1] Nicole L Wittwer,[1,2] Briony L Gliddon,[4] Melinda N Tea,[4] Rebecca Ormsby,[5] Santosh Poonnoose,[5,6] Jake Nowicki,[5,6] Orazio Vittorio,[7,8] David S Ziegler,[7,8,9] Stuart M Pitson,[3,4] Michael P Brown [1,2,3]

To cite: Gargett T, Ebert LM, Truong NTH, *et al*. GD2-targeting CAR-T cells enhanced by transgenic IL-15 expression are an effective and clinically feasible therapy for glioblastoma. *Journal for ImmunoTherapy of Cancer* 2022;**10**:e005187. doi:10.1136/jitc-2022-005187

► Additional supplemental material is published online only. To view, please visit the journal online (http://dx.doi.org/10.1136/jitc-2022-005187).

NTHT, PMK and KS contributed equally.

Accepted 13 September 2022

For numbered affiliations see end of article.

Correspondence to
Dr Tessa Gargett;
tessa.gargett@sa.gov.au

ABSTRACT

Background Aggressive primary brain tumors such as glioblastoma are uniquely challenging to treat. The intracranial location poses barriers to therapy, and the potential for severe toxicity. Effective treatments for primary brain tumors are limited, and 5-year survival rates remain poor. Immune checkpoint inhibitor therapy has transformed treatment of some other cancers but has yet to significantly benefit patients with glioblastoma. Early phase trials of chimeric antigen receptor (CAR) T-cell therapy in patients with glioblastoma have demonstrated that this approach is safe and feasible, but with limited evidence of its effectiveness. The choices of appropriate target antigens for CAR-T-cell therapy also remain limited.

Methods We profiled an extensive biobank of patients' biopsy tissues and patient-derived early passage glioma neural stem cell lines for GD2 expression using immunomicroscopy and flow cytometry. We then employed an approved clinical manufacturing process to make CAR- T cells from patients with peripheral blood of glioblastoma and diffuse midline glioma and characterized their phenotype and function in vitro. Finally, we tested intravenously administered CAR-T cells in an aggressive intracranial xenograft model of glioblastoma and used multicolor flow cytometry, multicolor whole-tissue immunofluorescence and next-generation RNA sequencing to uncover markers associated with effective tumor control.

Results Here we show that the tumor-associated antigen GD2 is highly and consistently expressed in primary glioblastoma tissue removed at surgery. Moreover, despite patients with glioblastoma having perturbations in their immune system, highly functional GD2-specific CAR-T cells can be produced from their peripheral T cells using an approved clinical manufacturing process. Finally, after intravenous administration, GD2-CAR-T cells effectively infiltrated the brain and controlled tumor growth in an aggressive orthotopic xenograft model of glioblastoma. Tumor control was further improved using CAR-T cells manufactured with a clinical retroviral vector encoding an interleukin-15 transgene alongside the GD2-specific CAR. These CAR-T cells achieved a striking 50% complete response rate by bioluminescence imaging in established intracranial tumors.

Conclusions Targeting GD2 using a clinically deployed CAR-T-cell therapy has a sound scientific and clinical rationale as a treatment for glioblastoma and other aggressive primary brain tumors.

BACKGROUND

Aggressive primary brain tumors have a devastating impact on patients and their families because survival rates are low and treatment options are limited. Glioblastoma (GBM), the most lethal of adult gliomas, has a poor 5-year relative survival rate (less than 7% at 5 years) which has altered a little in over 30 years despite the use of the multimodal 'Stupp' protocol.[1] Recurrence following this treatment is virtually inevitable.[2]

New treatments for these devastating brain tumors represent a high unmet clinical need, and yet these patients have so far not seen much benefit from immune checkpoint inhibitor (ICI) therapy.[3] Chimeric antigen receptor (CAR)-T-cell therapy is the other transformative immunotherapy with multiple Food and Drug Administration (FDA)-approved products for patients with relapsed/refractory B cell malignancies,[4 5] sparking interest in applying this treatment to a wider range of other cancer types not susceptible to ICIs.[6] CAR-T-cell therapy is appealing for GBM because, unlike ICI therapy that requires endogenous tumor-reactive T cells, CAR-T-cell therapy relies on an exogenous supply of genetically modified T cells that can be empowered to counter adverse factors generated within the tumor microenvironment. CAR-T-cell therapy for GBM is at an early stage of clinical

development, with only four reported phase 1 trials[7–10] and reviewed in,[11] showing feasibility and safety in targeting the antigens, EGFRVIII, HER2 and IL-13Rα2, with some clinical and biologic evidence of antitumor activity in select patients.

Our chosen target, the glycolipid tumor antigen GD2, is overexpressed in tumors of neuroectodermal origin such as neuroblastoma and has long been a tumor antigen of therapeutic interest.[12 13] The 14g2a monoclonal antibody, from which our CAR single-chain variable fragment (scFv) derives, binds the galactose, N-acetylgalactosamine, and sialic acid regions of the sugar moiety specific to the GD2 molecule.[14] Dinutuximab, the chimeric mAb sharing the same antigen binding domain as the 14g2a scFv, is an FDA-approved consolidation therapy for neuroblastoma.[15] We and colleagues have investigated third-generation GD2-CAR T cells as treatment for melanoma, neuroblastoma and other solid cancers.[16 17]

A study by Mount *et al* has shown high-level GD2 expression in diffuse midline glioma (DMG), an aggressive primary midline glioma in children[18] and, in a preclinical model, successful targeting by GD2-CAR-T cells. This served as rationale for a first-in-human study in patients with pediatric DMG, and data related to the first four treated patients were published recently.[19] Expression of GD2 in GBM has been reported previously in a study of primary cell lines,[20] however expression data direct from patient-derived GBM tissues are limited, and the study of GD2-targeted therapies in GBM is also limited. In recent publications, investigators have targeted glioma using anti-GD2 mAb therapy[20 21] or GD2-specific CAR-expressing mesenchymal progenitor cells.[22] In addition, murine GD2-specific CAR-T cells cleared a GD2-expressing murine glioma cell line in a syngeneic, immunocompetent mouse model, but only when used in combination with radiotherapy.[23] In a recent preclinical report of GD2-CAR-T-cell therapy in an intracranial model of human GBM, intratumoral administration was effective whereas intravenous administration was ineffective.[24] In addition, this study used a GD2-CAR derived from a monoclonal antibody with no reported cross-reactivity with mouse GD2, thus preventing the investigators from assessing off-tumor, on-target neurotoxicity.

Here we have validated GD2 as a promising clinical target in adult GBM. As an essential proof-of-principle before clinical trials commence, we have also shown that CAR-T cells can be successfully manufactured from peripheral blood mononuclear cells drawn from patients with GBM or diffuse intrinsic pontine glioma (DIPG), despite the perturbations that we have observed in the immune compartment of these patients. After GD2-CAR-T-cell administration, distinct patterns of tumor infiltration and control were observed in mice, allowing us to uncover tumor microenvironmental factors that may determine the effectiveness of the CAR-T-cell therapy. These findings support our clinical investigation of GD2-CAR-T in patients with GBM and DMG (Human Research Ethics Committee approved, #ACTRN12622000675729), but also indicate ways to further tailor CAR-based therapies to the unique GBM microenvironment.

RESULTS

GD2 is highly expressed in GBM tissues and in glioma neural stem cells derived from patient tissue

We first sought to comprehensively profile GD2 expression in GBM, as published reports of expression levels are limited,[20 25 26] using the same 14g2a antibody clone from which our CAR is derived. To this end, we used an extensive collection of human tumor tissues obtained from the South Australian Neurological Tumor Bank (SANTB) (a summary of patient material used in this study can be found in online supplemental table 1). From this primary human material, we analyzed both fresh frozen GBM tissue taken at surgical resection and glioma neural stem (GNS) cell lines established as previously described.[27] Importantly, the GNS lines were analyzed at early passage number (<10 for Centre for Cancer Biology (CCB)-annotated lines, and <25 for lines obtained as a kind gift from Professor Bryan Day, Queensland Institute of Medical Research Berghofer) and maintained in serum-free media that promote their stem-like state. We found high levels of GD2 expression in all assessed primary patient tissue (n=16) with variable levels of expression in different GBM tissue regions (figure 1A,B). ImageJ was used to independently assess staining intensity and confirm our observation of elevated GD2 staining in all GBM samples compared with tissue identified by the neurosurgeon as adjacent normal brain at the time of resection, which was statistically significant for paired samples (p=0.043, online supplemental figure 2A). To complement this investigation, we performed an analysis of public data sets online supplemental figure 2C,D, for the 2-gene signature of GD2 and GD3 synthase enzymes (*B4GALNT1* and *ST8SIA1*) which are predictive of GD2 expression[28] GBM (and low-grade glioma) have the highest level of the 2-gene signature among all cancer types in The Cancer Genome Atlas (online supplemental figure 1C). Although normal brain also has high levels of GD2 synthase, it lacks strong expression of GD3 synthase (online supplemental figure 1D). In keeping with this, direct staining of patient-derived tissues indicates low-level expression in non-malignant regions (figure 1A, online supplemental figure 2A,B). Early-passage GNS cells were also highly GD2-positive (17 of 20 lines, figure 1C,D and online supplemental figure 1B). We did not observe significant GD2 expression on the tissue-culture adapted cell lines, U87 and U251.

Diffuse Intrinsic Pontine Glioma (DIPG, now reclassified as DMG, Diffuse Midline Glioma) has been reported by others to have extremely high GD2 expression.[18] As surgical resection is precluded, we obtained four needle biopsy and four autopsy samples from children with DIPG and confirm enhanced GD2 expression in H3 K27M mutant DIPG (online supplemental figure 2C,D). We also confirmed GD2 expression was maintained when an early

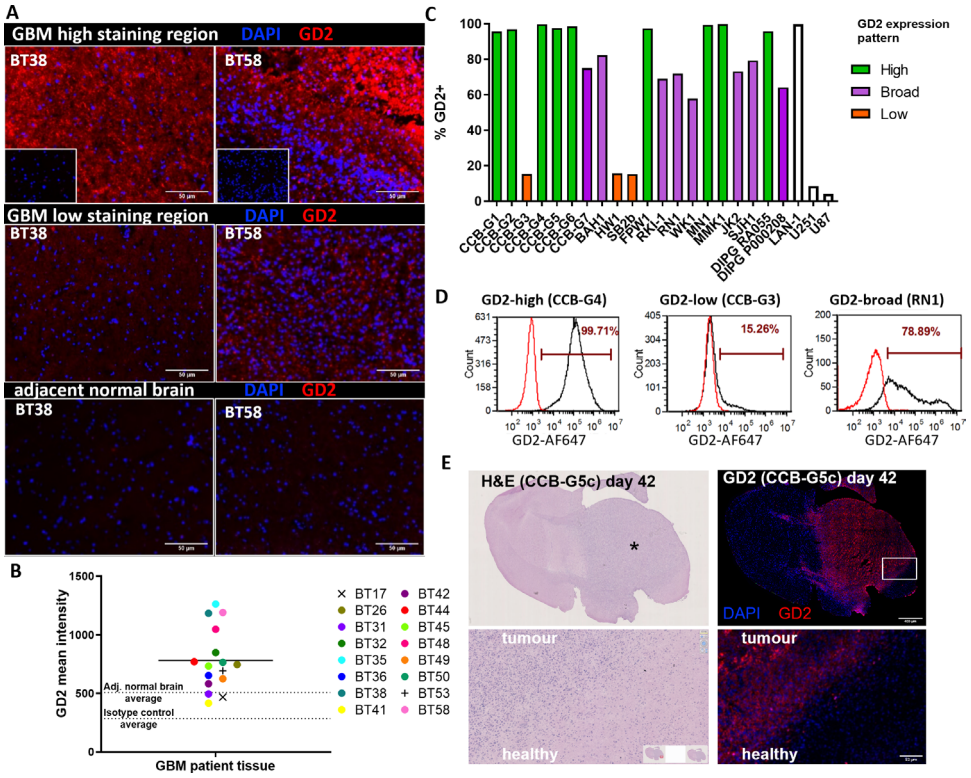

Figure 1 High-level GD2 expression in glioblastoma (GBM) tumor tissues and glioma neural stem (GNS) cell lines, but not in normal brain. (A) Sections of surgical specimens from GBM (n=16) or surrounding non-involved brain (n=4) were stained by immunofluorescence using an anti-GD2 primary antibody (clone 14g2a) and IgG2a isotype control antibody (top row insets). Representative staining for regions of high (top) and low (middle) GD2 expression, and matched adjacent normal brain tissue (bottom). (B) Summary of GD2 staining intensity measured by ImageJ. Dotted lines at y-axis mark average staining intensity for (1) adjacent normal brain tissue (n=4) removed by neurosurgeon to access the tumor, and (2) the isotype control. (C) Summary of GD2 expression on GNS cell lines, which were generated from patients with GBM and DIPG's tumors and maintained in culture for <25 passages. (D) Representative histograms showing the three distinct GD2 expression patterns observed. Cells were analyzed by flow cytometry for GD2 expression using anti-GD2 primary mAb (clone 14g2a; black histograms) or isotype-matched control antibodies (red histograms). (E) The CCB-G5C GNS cell line was implanted in the brains of NOD-SCID-gamma-null (NSG) mice via stereotactic intracranial injection. Representative image of H&E staining (left) and GD2 immunofluorescence (right) of coronal section of mouse brain at time of humane killing because of neurological signs n=10, for full analysis of groups see figures 4–5. Asterisk marks side of tumor inoculation. CCB, Centre for Cancer Biology; DIPG, diffuse intrinsic pontine glioma.

passage GNS cell line (CCB-G5c) was established as an intracranial xenograft in NSG mice (figure 1E).

Thus, we found GD2 was strongly expressed on GBM and DIPG tissues, and GNS cells retained GD2 expression in an aggressive orthotopic xenograft model.

GD2-specific CAR-T cells can be manufactured from patient with GBM-derived T cells, but the peripheral immune compartment of these patients is significantly perturbed

Most CAR-T-cell therapy occurs in the autologous setting. However, an element often overlooked in preclinical CAR-T-cell development is the relative fitness of patient-derived T cells for CAR-T-cell manufacturing. In our experience, healthy donor-derived CAR-T cells typically have uniformly successful expansion and potent cytotoxic function, while patient-derived CAR-T cells can have more variable expansion and functional capacity because of patient-specific factors including age, prior treatment, concomitant administration of corticosteroids and disease status. Hence, we undertook an assessment of the suitability of patients with GBM and DIPG's peripheral blood as a starting point for manufacturing, following our established and approved clinical manufacturing protocol for generating third-generation (CD28-OX40-CD3ζ) GD2-CAR-T cells.[29] Donor characteristics are presented in online supplemental table 1, and products were compared with previously manufactured clinical products for patients with melanoma on the CARPETS trial (www.anzctr.org.au: ACTRN 12613000198729). DIPG/DMG pretreatment was limited to radiotherapy in most cases, whereas primary patients with GBM had no prior chemotherapy/radiotherapy but were all receiving oral corticosteroids at the time of blood donation.

Previously reported findings of lymphopenia, neutrophilia, and a profound decrease in eosinophils in patients with GBM[30–32] were recapitulated in our survey (figure 2A and online supplemental figure 3A-D). Furthermore, compared with patients with melanoma, a specific deficit in T cells and an inverted CD4:CD8 ratio, with

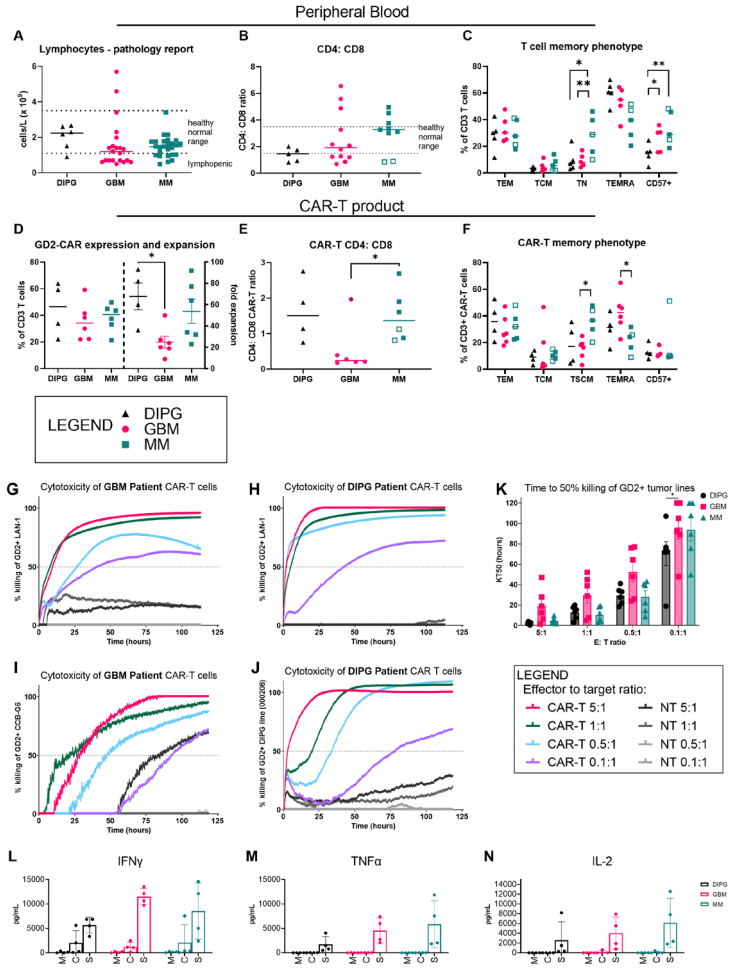

Figure 2 GD2-specific CAR-T cells can be manufactured from peripheral blood of patients with glioblastoma (GBM) and diffuse intrinsic pontine glioma (DIPG) and have a distinct phenotype. Immune phenotype of patient with GBM, DIPG, and metastatic melanoma (MM)-derived CAR-T cells as determined by multicolor flow cytometry. (A) Peripheral blood lymphocyte counts obtained at time of blood collection for CAR-T-cell manufacture. (B) Ratio of peripheral blood lymphocyte $CD4^+$ and $CD8^+$ T cells for each tumor type. Pathology service-defined healthy normal range is marked where available. (C) Proportions of various memory subsets within the peripheral T-cell population: effector memory ($CD45RA^-$ $CCR7^-$ $CD62L^-$); central memory ($CD45RA^-$ $CCR7^+$ $CD62L^+$); naïve ($CD45RA^+$ $CCR7^+$ $CD62L^+$); TEMRA ($CD45RA^+$ $CCR7^-$ $CD62L^{+/-}$). (D) Relative expression and expansion of GD2-CAR-T cells in vitro for each tumor type. (E) Ratio of $CD4^+$ and $CD8^+$ CAR-T cells. (F) Proportions of memory subsets within CAR-T cells, defined as for (C). Cytotoxicity against GD2-expressing tumor cell lines of neuroblastoma (LAN-1), GBM (CCB-G6) and DIPG (000208) as determined by a real-time cell adhesion-based assay. CAR-T cells derived from (G) patients with GBM (BT29) and (H) DIPG (DIPG1) were assayed against the LAN-1 neuroblastoma target cell line used for batch release testing in our clinical trials. CAR-T cells derived from (I) patients with GBM (BT29) and (J) patients with DIPG (DIPG1) were assayed against the matched glioma neural stem cell line (CCB-G6) and the unmatched DIPG cell line (000208), respectively. Representative data from one patient are shown; n=4 patient samples. (K) Summary data of all patient product cytotoxicity assays showing the time in hours to reach 50% killing of targets (KT50). Production of (L) IFN-gamma (M) TNF-alpha (N) IL-2 from CAR-T cell products from patients with DIPG, GBM or MM were cultured with media only (M), media plus IL-7 and IL-15 homeostatic proliferative cytokines (C), or media and plate-bound 1A7 antibody for CAR stimulation for 72 hours (S). Other cytokines, and cytokines from peripheral T cells directly isolated from patients are shown in online supplemental figure 5.; n=3 patient samples, two-way analysis of variance and Tukey's multiple comparison post-tests. CAR, chimeric antigen receptor; CCB, Centre for Cancer Biology; IFN, interferon; IL, interleukin; TNF, tumor necrosis factor.

lower $CD4^+$ T cells relative to $CD8^+$ T cells, was observed both for patients with GBM and DIPG in support of a recent report of CD4 T-cell bone-marrow sequestration observed with intracranial tumors (figure 2B).[33] Of note, two patients with melanoma with brain metastases had a similarly perturbed CD4:CD8 ratio (open squares). When T-cell immune-phenotyping was performed, significant reductions in the naïve T cell ($CCR7^+$, $CD62L^+$ and $CD45RA^+$) compartment were observed for patients with DIPG and GBM compared with patients with melanoma (figure 2C and online supplemental figure 3E).

Nevertheless, CAR-T-cell manufacturing was achieved for each of six selected patients with GBM and five selected patients with DIPG/DMG, with transduction

efficiencies and cell expansion yields sufficient to meet our protocol-defined batch release criteria (figure 2D). Cell expansion for several adult patient with GBM-derived CAR-T-cell products was however slower than that reached for our CARPETS trial patients with melanoma. Finally, the CD4:CD8 ratio of CAR-T-cell products generally matched that observed in patients' peripheral blood samples and had a lower proportion of $CD4^+$ T cells (figure 2E). Although our culture conditions are optimized for maintaining a central memory phenotype to promote survival and persistance,[29 34] a smaller proportion of the patient with GBM-derived CAR-T-cell product was classified as central memory, and a higher proportion had a heterogenous TEMRA phenotype compared with patient with melanoma-derived CAR-T cells (figure 2F and online supplemental figure 3E).

To assess the function of CAR-T cells in vitro, we co-cultured a range of $GD2^+$ tumor cell lines with CAR-T cells in a real-time impedance-based cytotoxicity assay over 5 days. CAR-T cells manufactured from patients with GBM (figure 2G,I) and patients with DIPG (figure 2H,J) effectively killed $GD2^+$ cells of the neuroblastoma line, LAN-1, and cells of either early-passage GNS and DIPG lines. We use the level of LAN-1 cytotoxicity as a CAR-T-cell manufacturing batch release criterion, which all products met. Importantly, the GBM tumor line was efficiently killed by CAR-T cells manufactured from the same donor patient with GBM. Killing was also achieved at low effector:target ratios of 1 CAR-T cell to 10 tumor cells, indicating high potency T cells capable of sequential, antigen-specific killing[35] or a bystander killing effect. DIPG-derived CAR-T cells were particularly potent, with the shortest time to 50% killing at this lowest ratio (figure 2K).

Cytokine production from stimulated CAR-T cells from patients with GBM and DIPG/DMG indicated they secreted multiple effector cytokines including interferon-γ, tumor necrosis factor-α and interleukin (IL)-2, and did so at a comparable level to CAR-T cells manufactured from our patients with melanoma (figure 2L–N). Immune-suppressive cytokines IL-10 and Transforming Growth Factor beta (TGF-β) were undetectable (not shown), however inflammatory cytokines such as IL-17A, IL-6 and IL-8 were also significantly produced, most markedly from the patient with DIPG-derived CAR-T cells and this matched what was seen for peripheral T cells sorted directly from blood of these patients (online supplemental figure 4).

Therefore, these data show that although patient with GBM-derived CAR-T cells had a distinct phenotype, and expanded more slowly, they performed well in vitro in functional assays of cytotoxicity and cytokine secretion.

GD2-specific CAR-T cells control orthotopic xenografts of GBM

To determine CAR-T activity in vivo we employed an orthotopic xenograft model. In this model, NSG mice receive an intracranial injection of an early-passage patient-derived GNS cell line carrying a luciferase reporter gene *via* stereotactic delivery to the right brain hemisphere (figure 3). The CCB-G5c line was selected for its rapid growth kinetics, which cause neurological signs such as head-tilt and altered gait between days 35 and 42. These clinical signs are used, in part, as endpoints for humane killing. We sought to compare treatment with healthy donor-derived CAR-T cells versus patient with GBM-derived CAR-T cells to determine whether differences in their in vivo fitness and tumor control were evident.

Bioluminescence imaging (BLI) revealed a delayed increase in luminescence signals for mice treated with GD2-CAR-T cells from healthy donors (HV CAR-T) or patients with GBM (GBM CAR-T) compared with controls: untreated mice or mice treated with non-transduced T cells (NT-T) (figure 3A,B). Survival was significantly longer in CAR-T-treated mice (mean 52 days, HV CAR-T and 53 days, GBM CAR-T) compared with untreated or NT-T treated mice (each mean, 42 days) (figure 3C). CAR-T-treated mice were also less likely to display neurological signs and were more frequently euthanized because of poor body condition or weight loss or both, which were the other endpoint criteria for the study (figure 3D). Here, we note that these constitutional signs may be disease-related or treatment-related because NSG mice are susceptible to graft versus host disease (GvHD) with GvHD onset reported at 4–6 weeks in other studies.[18] Importantly, no CAR-T-cell treated mice were killed for neurological signs before the control tumor-bearing mice, consistent with a lack of GD2-CAR-T-cell-mediated neurotoxicity, which had been observed in other studies of GD2-CAR-T-cell therapy as early as day 7 post infusion.[18 36] We employed independent clinical and veterinary pathologists to evaluate histopathologic samples from the xenograft tumors and normal mouse brain tissue, respectively (figure 3E) with no abnormal findings reported for normal brain tissues. Sham-operated mice, which received an intracranial injection of saline, were also treated with CAR-T cells to assess whether neurotoxicity was evident in the absence of tumor and no pathologic signs were detected (figure 3Ei)

Accordingly, although we could show that both healthy and patient with GBM-derived GD2-CAR-T cells slowed GBM growth and did not contribute to on-target, off-tumor neurotoxicity, the treatment was not curative in this model. We hypothesized that one, or more of the following, were the likely cause for the tumor escaping CAR-T control: (1) insufficient CAR-T homing to and infiltration of the tumor, (2) insufficient CAR-T-cell function because of intrinsic T-cell defects or extrinsic tumor microenvironmental factors, or (3) rebound growth of GD2-negative tumor. To determine which factors contributed to immune escape, we next undertook a detailed analysis of the brain tissues using multicolor immunofluorescence and flow cytometry.

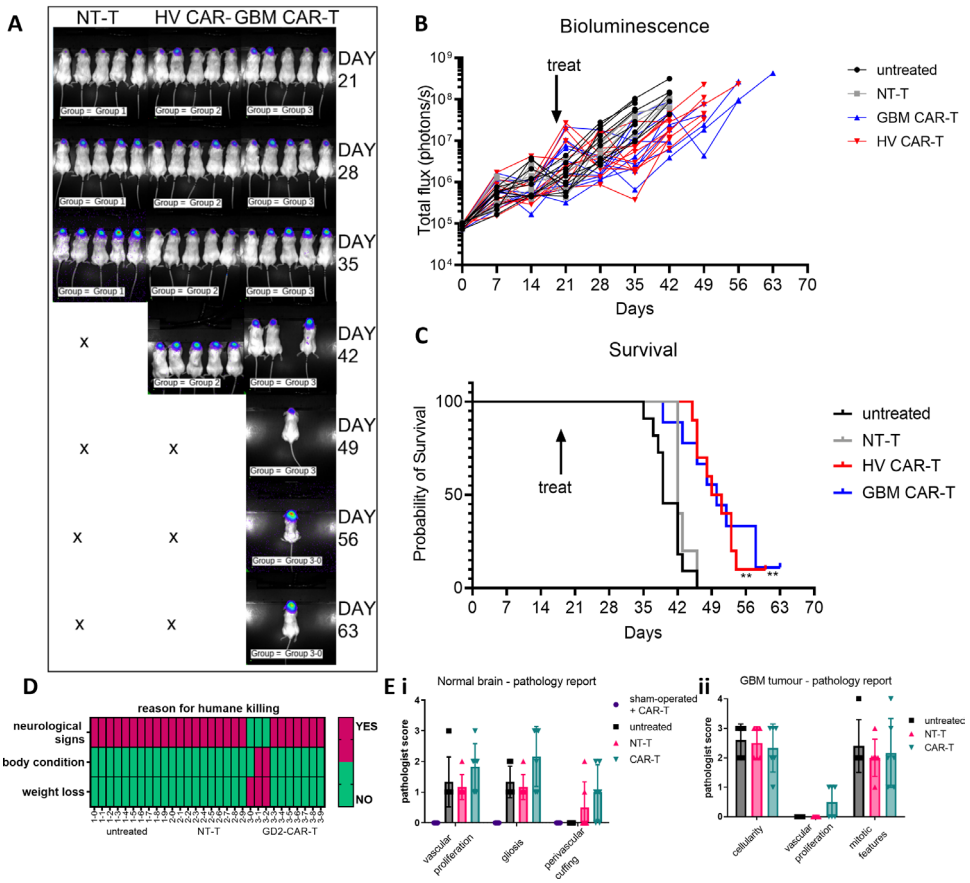

Figure 3 Third-generation GD2-CAR T cells control orthotopic GBM xenografts but do not adversely affect the normal mouse brain. Mice received 2×10^5 Centre for Cancer Biology-G5c cells by stereotactic intracranial injection on Day 1. On Day 17, mice were given single intravenous injections of saline (untreated), 1.5×10^6 non-transduced control T cells from a healthy donor (NT-T), 1.5×10^6 healthy donor-derived GD2-CAR-T cells (HV CAR-T), or 1.5×10^6 patient with GBM-derived GD2-CAR-T cells (GBM CAR-T, from donor BT11 or donor BT48, unmatched to the xenograft). n=8–10/group. (A) Representative bioluminescence imaging (BLI) for NSG mice with intracranial GBM xenografts. (B) BLI data for all mice. (C) Kaplan-Meir survival curves and statistics for mice. Statistics shown are from individual Gehan-Breslow-Wilcoxon tests comparing each curve to the untreated curve. (D) Clinical signs resulting in humane killing according to predefined criteria (see Methods). Mice humanely killed for neurological signs also routinely displayed weight loss, reluctance to move and ruffled coats, however these alone did not reach a severity score requiring euthanasia. (E) Independent histopathology scoring of brain sections from humanely killed mice of the (i) remaining normal brain tissue and (ii) GBM tumor. Abnormal features were graded as: 0=none; 1=minimal; 2=moderate; 3=severe. Cellularity was graded as: 1=low; 2=moderate; 3=dense. Mitotic features were reported as number per field of view. CAR, chimeric antigen receptor; GBM, glioblastoma.

Distinct patterns of CAR-T-cell tumor infiltration and CD31$^+$ vessel formation at study endpoints correlate with survival

Immunofluorescence staining for GD2 showed that in most (9 of 11) CAR-T-treated mice, GD2 was still abundantly expressed in the tumor, ruling out tumor antigen loss as a reason for immune escape in most mice (figure 4). Nevertheless, the single longest-surviving mouse, which had a notable number of human CD3$^+$ tumor-infiltrating T cells (figure 4A; iv), also had the lowest level of tumor GD2 expression but with a strong tumor bioluminescence signal, indicating that in this case, GD2-negative or GD2-low tumor cells had resulted in tumor regrowth (figure 4A–C).

Analysis of human CD3$^+$-stained tumor-infiltrating T cells revealed marked variations in the extent of T-cell infiltration at study endpoints. T-cell infiltration in treated mice was graded as low/negative, intermediate, or high (T-cell inflamed) (figure 4A–C). Of note, high levels of CD3 staining correlated with the longest survival (R^2 0.6375, p=0.0004).

Staining for mouse CD31 highlighted the abundance of microvessels within the tumor. It also showed T cells surrounding larger, structured vessels, consisting of strong CD31 staining around a defined lumen, and there was a significant positive correlation between numbers of these large vessels and survival (R^2 0.4583, p=0.0056, figure 4A–C). Large vessels within the GBM xenograft were not observed in untreated mice, suggesting this was not a tumor-intrinsic feature, but a feature resulting from CAR-T-cell interactions within the tumor microenvironment. Staining for mouse myeloid lineage cells (CD45, F4-80, CD11b, CD11c, GR-1) detected a minor population of mouse macrophages in the xenograft tumor (average ~3% of viable cells (not shown), compared with

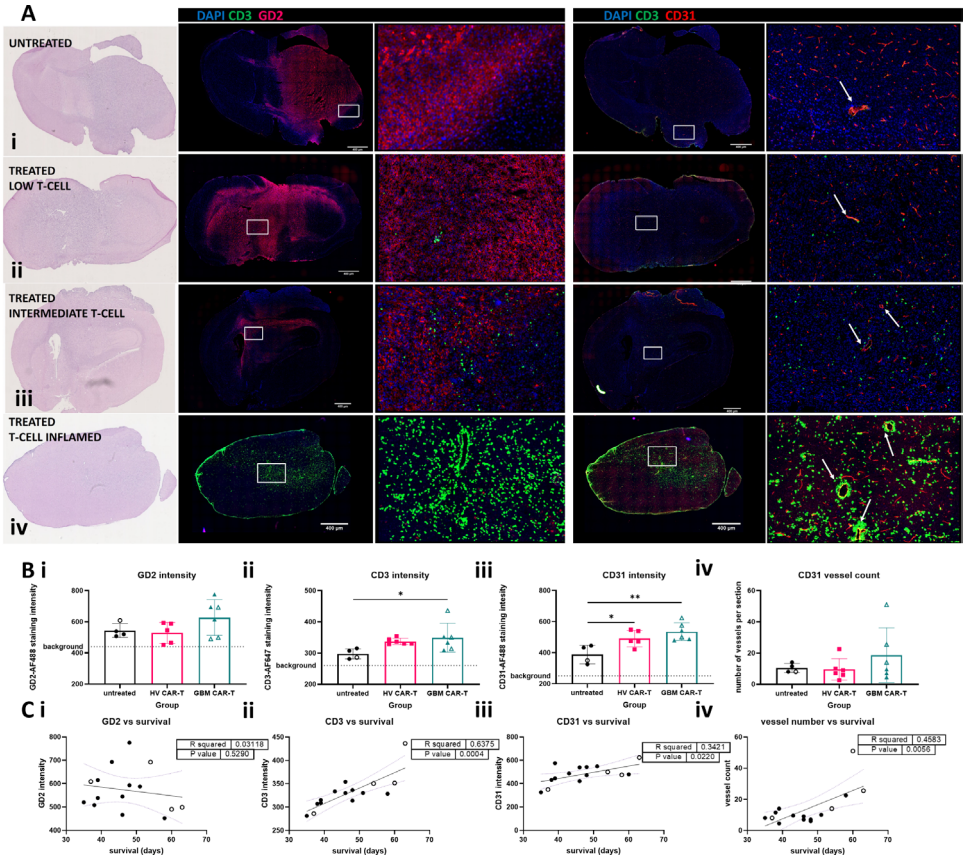

Figure 4 T-cell infiltration as shown in whole brain sections and dissociated tissue samples. At the time of humane killing, mouse brains were bisected, and half was reserved for immunofluorescence (IF) staining of whole tissue, and half was dissociated for flow cytometric analysis alongside spleen and bone marrow. (A) Whole brain sections (mid-coronal plane where possible) were assessed by H&E staining (far left column), and IF using anti-GD2-AF488 (clone 14g2a) and anti-human CD3 AF647 (columns 2 and 3) or anti-human CD3-AF647 and anti-mouse CD31-AF488 (columns 4 and 5) antibodies. White boxes on the whole brain sections indicate regions of interest shown at higher magnification (40×) to the right. White arrows indicate large vessels, identified by the presence of a black lumen and distinct from microvessels. Representative images from (i) an untreated mouse, and three GBM CAR-T treated mice (ii–iv) have been chosen to show the range of staining for each molecule. n=6/group. (B) ImageJ analysis of the staining intensity for GD2, CD3 and CD31 (i–iii), and enumeration of the number of large $CD31^+$ vessels (iv). Statistical analysis by two-way analysis of variance (ANOVA) and Tukey's multiple comparison post-tests. The individual mice represented in the IF microscopy images are shown with open symbols. (C) Linear regression analysis of staining intensity (i–iii) or large vessel number (iv) versus survival time of mice. statistical analysis with two-way ANOVA and Tukey's multiple comparison post-tests. See online supplemental figure 5 for flow cytometric analysis of CAR+T cells, with absolute counts, representative dot plots and statistical analysis of the correlation between absolute cell numbers and survival. CAR, chimeric antigen receptor; GBM, glioblastoma.

the expected proportion of ~30–50% macrophages in human GBM).[27] Thus, the immune suppressive macrophage population that is abundant in human GBM is not well represented in this model.

Next, tissue-infiltrating CAR-T cells were directly assessed by flow cytometry using the anti-idiotypic 1A7 antibody specific for the CAR antigen binding domain.[37] CAR-T cells were detected in brain, spleen, and bone marrow by flow cytometry, confirming successful homing and engraftment (online supplemental figure 5A-C). We noted that patient with GBM-derived CAR-T-cell therapy resulted in significantly higher absolute numbers of CAR-T cells in the brain, although this did not result in improved survival in these mice compared with mice treated with healthy donor-derived CAR-T cells.

Necropsies were done mainly at humane killing endpoints and thus may not adequately capture the dynamics of interactions between CAR-T cells and tumor. Hence, to further evaluate the association of these findings with survival of tumor-bearing mice, treated mice were split into two groups based on survival times (short-term and long-term survivors, see online supplemental figure 5A). Although absolute CAR-T-cell numbers varied substantially within each group, overall, higher numbers of $CD3^+$, $CD4^+$ and $CD8^+$ CAR-T cells within the brain were significantly associated with longer survival (online supplemental figure 5D) and long-term survivors had significantly higher numbers of $CD3^+$ CAR-T cells in bone marrow.

Thus, intravenously administered GD2-CAR-T cells were able to engraft peripherally and access the brain tumor, and these findings were linked with longer overall survival in tumor-bearing mice.

Expression of an IL-15 transgene significantly improves CAR-T engraftment and tumor control

CAR-T-cell engraftment is a known and strong correlate of its clinical effectiveness. Here, although we found that GD2-CAR-T-cell engraftment and infiltration of the brain correlated with improved survival, persistence of GD2-expressing tumors suggested insufficient immune selection pressure or countervailing tumor microenvironmental factors, or both, in most mice. We considered ways to further improve tumor control including simply increasing CAR-T-cell dose in mice (ie, from the 10^6 range to the 10^7 range) but this would exceed the equivalent cell dose that would be practicable in patients. Alternatively, administration of a similar dose of CAR-T cells engineered to have a greater proliferative potential may achieve the same end as a higher cell dose. To this end, we considered a clinically relevant GD2-CAR-T retrovector also encoding secreted human IL-15.[38–40] We obtained a second-generation GD2-CAR retrovector co-expressing human IL-15 (kindly supplied via Baylor College of Medicine and shown in online supplemental figure 6A). This vector consists of an identical scFv, CD3ζ and CD28 domains, and the same inducible Caspase 9 suicide gene, but is distinguished by hinge and transmembrane domains from CD8α and a lack of OX40. Like the third-generation GD2-CAR retrovector that we and our collaborators have used in the CARPETS and GRAIN clinical studies,[16 17] a highly similar second-generation GD2-CAR-IL-15 retrovector, which also contains an extended VH-VL interdomain linker in the CAR,[38 39] is being used in active clinical studies (ClinicalTrials.gov: NCT03294954; NCT03721068), and therefore represents a strong candidate for phase 1 testing in GBM and DIPG.

We first performed in vitro characterization of GD2-CAR-IL-15 T cells derived from healthy volunteers and patients with GBM (online supplemental figure 6B-E) to confirm functionality before assessment in the intracranial xenograft model.

When mice were treated with healthy donor-derived GD2-CAR-T cells enhanced with the IL-15 transgene, highly effective GBM tumor control was observed, with a mean survival of 63.5 days (figure 5). Mice treated with the third-generation GD2-CAR-T cells (lacking IL-15 enhancement) had a mean survival of 47 days and, similar to the previous experiment, the mean survival times for control mice were 41 and 42 days for untreated and NT-T cell treated mice, respectively (figure 5A,B). In three of six mice treated with GD2-CAR-IL-15-T cells, the bioluminescence signal was undetectable between days 49 and 63. However, at the final time point (day 67), a recrudescent low-level bioluminescence signal suggested some tumor regrowth. Therefore, all remaining mice were culled to allow an ex vivo assessment of tumor burden and CAR-T-cell infiltration. As GD2-CAR-IL-15-T cells were more often culled because of poor body condition rather than neurological signs (figure 5C) and had markedly enlarged spleens (online supplemental figure 7A), we suspected GvHD, as reported by others.[18] As with the previous experiment, CAR-T-cell treated mice did not show early onset of neurological signs compared with control mice, and there was no evidence of off-tumor CAR-T cell-mediated neurotoxicity (figure 5C).

Brain tissues from two individual mice from each treatment group were used for bulk next-generation RNA sequencing to provide a transcript-level overview of changes in the tumor microenvironment between groups (selected gene signatures in figure 5D and unbiased analysis in online supplemental figure 8). Tissue from GD2-CAR-IL-15-T-cell-treated mice had the most dramatic changes in their transcriptome, with over 2000 genes significantly up or down regulated, compared with untreated controls. These mice had higher transcript levels of some chemokine receptors associated with tumor homing (CCR5, CXCR6, CX3CR1)[41] and cytotoxic mediators (PRF and GZMA, GZMH and GZMK), compared with GD2-CAR-T-cell-treated mice, indicating differences in homing and cytolytic potential. The mice treated with the third-generation GD2-CAR-T cells had notably higher levels of transcripts associated with a vasculature permissive to T-cell extravasation (mouse Pecam1, Sele and Selp), compared with all other groups.

At study endpoints, GD2 staining was high in the tumors of control mice (untreated and NT-T treated), and lower in all CAR-T-treated mice (figure 5E,F), The CD3 staining intensity in brain was highest for third-generation GD2-CAR-T-treated mice. However, unlike in the previous experiment, a linear regression analysis showed that the CD3 staining intensity did not correlate with survival because in this experiment long-term survivors among GD2-CAR-IL-15-T-treated mice had intermediate intensity of CD3 staining (figure 5F,G). Although $CD31^+$ vessels were again highest in the CAR-T-treated mice, mice with higher numbers of CD31 vessels did not always survive longest, unlike in the previous experiment (figure 5F,G). Of note, a mouse in the GD2-CAR-T-treated group was a clear outlier, culled on day 42 despite having significantly high levels of $CD31^+$ vessels and human $CD3^+$ cell infiltration in the brain (represented in figure 5, ii). The mouse was culled for poor body condition and significantly skews the survival analysis and correlative analysis of CD31 vessels. If excluded from the data set, it restores the significance in line with the previous experiment (see online supplemental figure 7H,I).

Flow cytometry analysis of dissociated tissues confirmed the presence of GD2-CAR-expressing T cells in the brain, spleen, and bone marrow (online supplemental figure 7C-G). As we had observed in the CD3 immunofluorescence analysis, the third-generation GD2-CAR-T-treated mice had significantly higher numbers of CAR-positive T cells in the brain compared with the GD2-CAR-IL-15-T-treated mice. The latter mice had significantly higher

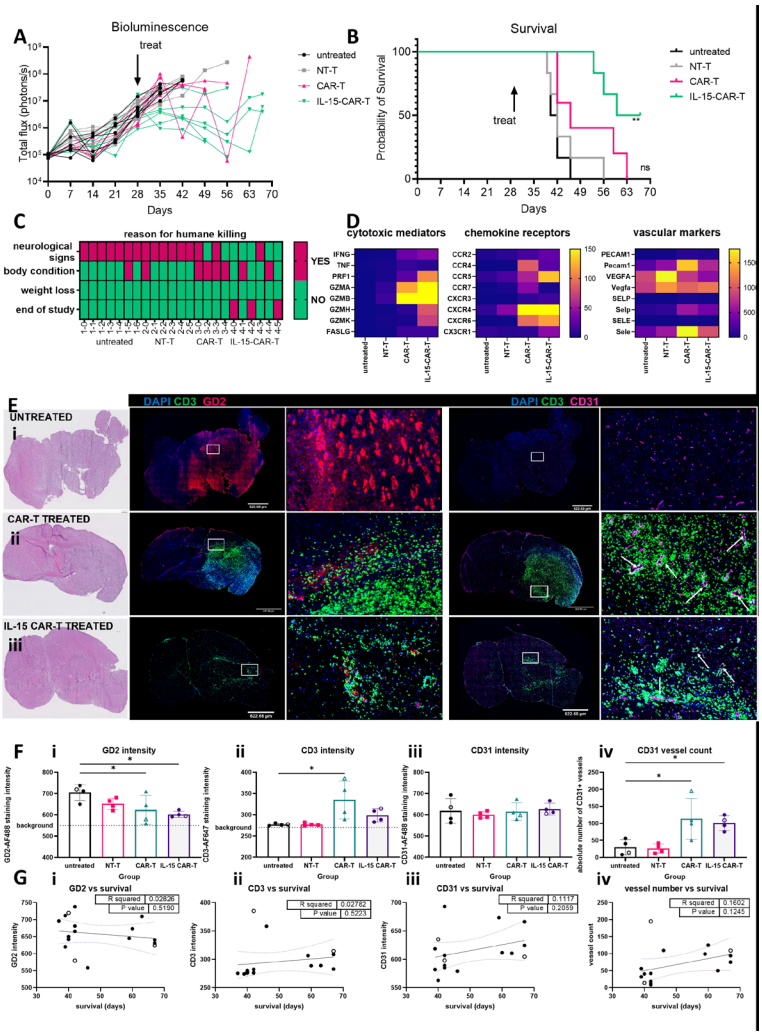

Figure 5 Incorporating an IL-15 transgene confers superior orthotopic tumor control by second-generation GD2-CAR-T cells compared with third-generation GD2-CAR-T cells. Mice received 2×10^5 Centre for Cancer Biology-G5c cells by stereotactic injection on Day 1. On Day 28, mice were given single intravenous injections of saline (untreated) 1.5×10^6 non-transduced control T cells (NT-T) from healthy donor, 3×10^6 healthy donor-derived third-generation GD2-CAR T cells (CAR-T) or 3×10^6 IL-15-containing GD2-specific CAR-T cells (IL-15-CAR-T). n=5–6/group (A) BLI data for all mice. (B) Kaplan-Meir survival curves and statistics for mice. Statistics shown are from individual Gehan-Breslow-Wilcoxon tests comparing each curve to the untreated curve. (C) Clinical signs resulting in humane killing according to predefined criteria (see Methods). (D) Next-generation sequencing of whole brain dissociated tissues from two untreated, two NT-T treated, two CAR-T treated and two IL-15-CAR-T treated mice. Heatmap of selected markers show average normalized messenger RNA counts (Reads per KB per million). (E) Whole brain sections (mid-coronal plane where possible) were assessed by H&E staining (far left column), and immunofluorescence (IF) using anti-GD2-AF647 (clone 14g2a) and anti-human CD3 AF488 (columns 2 and 3) or anti-human CD3 AF488 and anti-mouse CD31-AF647 (columns 4 and 5) antibodies. White boxes on the whole brain sections indicate regions of interest shown at higher magnification to the right. White arrows indicate large vessels, identified by the presence of a black lumen and distinct from microvessels. Representative images from an (i) untreated mouse, (ii) CAR-T treated mouse, and (iii) an IL-15-containing CAR-T-treated mouse have been chosen to show the range of expression for each molecule. n=4/group, statistical analysis by two-way analysis of variance (ANOVA) and Tukey's multiple comparison post-tests. (F) ImageJ analysis of the staining intensity for each antibody (i–iii), and enumeration of the number of large $CD31^+$ vessels (iv). The individual mice represented in the IF microscopy images are shown with open symbols. (G) Linear regression analysis of IF staining and survival, statistical analysis with two-way ANOVA and Tukey's multiple comparison post-tests. CAR, chimeric antigen receptor; IL, interleukin.

numbers of CAR-positive T cells in the spleen, although the numbers of CAR-positive T cells in bone marrow in both groups of CAR-T-treated mice were equivalent.

Together these data suggest that the two different GD2-CAR-T-cell products have different engraftment and homing potentials. Compared with the third-generation GD2-CAR-T cells, the antitumor effectiveness of GD2-CAR-IL-15-T cells appears to depend less on absolute numbers in the brain and suggests that these CAR-T cells have a distinct biology and employ unique mechanisms to achieve tumor control.

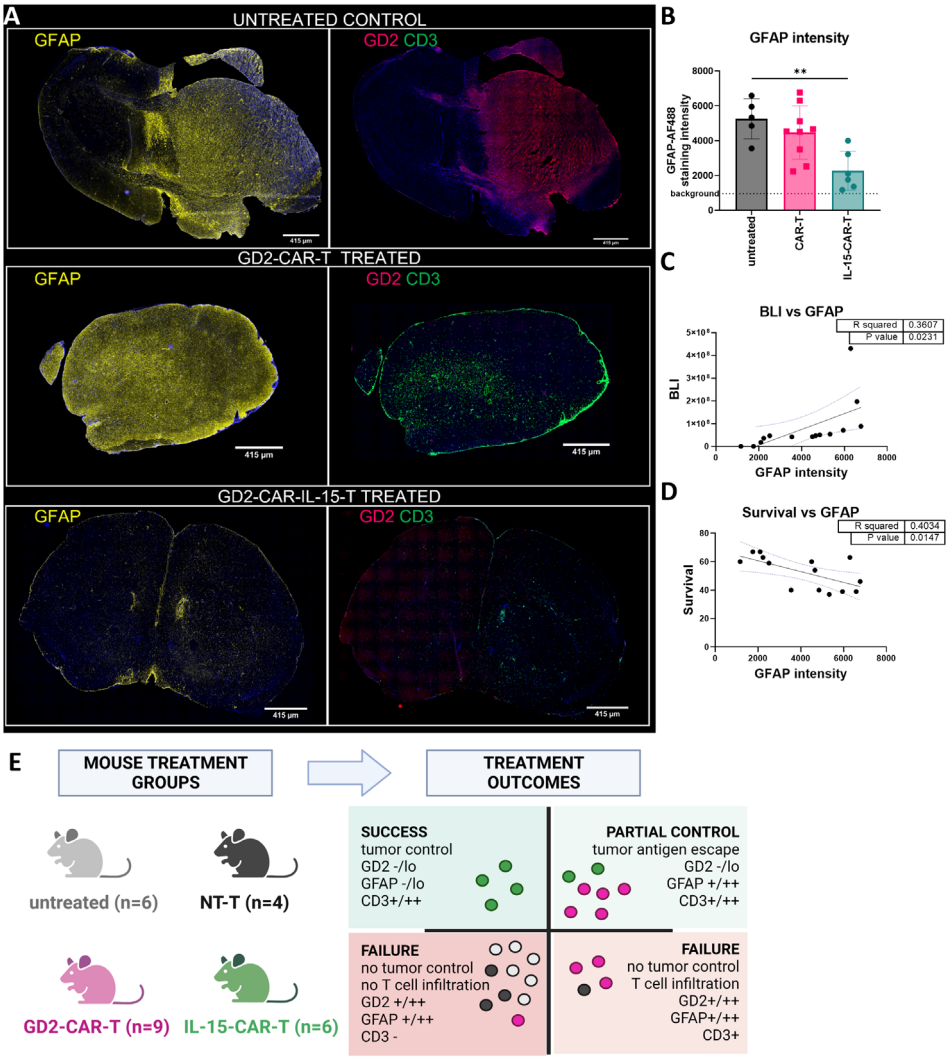

Figure 6 Staining for human GFAP reveals the extent of tumor control versus tumor escape. (A) Whole brain sections were stained with rabbit anti-human GFAP. Contiguous sections stained with GD2 and CD3 are presented alongside to enable direct comparison. Representative images from (i) untreated mouse, (ii) GD2-CAR-T treated mouse, and (iii) GD2-CAR-IL-15 treated mouse. n=6–8/group. See also online supplemental table 2 for a full data summary. (B) ImageJ analysis of the staining intensity for human GFAP antibody, statistical analysis with two-way analysis of variance and Tukey's multiple comparison post-tests The individual mice represented in the IF microscopy images are shown with open symbols. Linear regression analysis of GFAP IF staining and (C) GD2 staining intensity (D) bioluminescence (BLI—total flux) at endpoint (E) survival (days). BLI, bioluminescence imaging; CAR, chimeric antigen receptor; IL, interleukin; IF, immunofluorescence; NT-T, non-transduced T cells.

Analysis of tumor marker GFAP reveals distinct patterns of tumor control and escape

During our staining analysis of both experiments we identified numerous mice with high $CD3^+$ infiltrates and low GD2 expression, indicating destruction of $GD2^+$ tumor. However, some of these mice still had a significant bioluminescence signal, indicating possible outgrowth of a $GD2^-$ tumor. Hence, we undertook an assessment using the tumor marker, human GFAP, which is highly expressed in our patient-derived GNS lines (figure 6A,B). GFAP staining intensity correlated well with BLI and had an inverse relationship with survival (figure 6C,D). Mice in the GD2-CAR-IL-15-T treatment group had significantly lower GFAP staining, consistent with the observed reduction in bioluminescence signal for this group and indicating significantly decreased tumor volumes, compared with other treated mice or untreated control mice (figure 6B). The distinct patterns of CD3, GFAP and GD2 expression at endpoint allowed us to classify mice in the following groups: (i) successful tumor control with $CD3^+$ infiltrates and limited residual tumor (BLI^{low}, $GD2^{-/low}$ and $GFAP^{low}$); (ii) partial tumor control preceding GD2 antigen loss and tumor escape with $CD3^+$ infiltrates and substantial tumors (BLI^{high}, $GD2^{-/low}$ and $GFAP^{high}$), and (iii) unsuccessful treatment with substantial $GD2^+$ tumors remaining (BLI^{high}, $GD2^{high}$ and $GFAP^{high}$). These

classifications summarized in figure 6E, and full results are presented in online supplemental table S2. Examples of mice with a reduction followed by a rebound in the bioluminescence signal are shown in online supplemental figure 9.

DISCUSSION

This is the first study to validate a clinically relevant GD2-CAR-T-cell product as a therapy for GBM. Importantly, in this study we have used patients' blood samples for CAR-T-cell manufacture and patients' tissues to establish early-passage GNS cell lines as CAR-T-cell targets and to generate orthotopic tumors. Hence, in contrast to prior preclinical studies using tissue culture-established tumor cell lines and healthy donor-derived CAR-T cells, we have evaluated this CAR-T-cell therapy by also considering the state of the tumor and immune compartments in patients with GBM.

GD2 has long been a tumor-associated antigen of interest.[12] Here, we reveal high-level GD2 expression on surgical biopsies. However, as with all tumor-associated antigens, care must always be taken to consider patterns of expression on healthy tissues because of the known on-target, off-tumor toxicities of CAR-T-cell therapies. As a normal tissue antigen, the neuronal expression of GD2 is an apparent concern for the treatment of $GD2^+$ malignancies in the brain, which is encased in the confined space of the skull and thus less able to tolerate potential immune-inflammatory reactions of CAR-T-cell therapy.

As the donor of the same antigen binding region as US FDA-approved dinutuximab,[15] the 14g2a mAb also supplies the scFvs employed in GD2-CARs of this study. Of note, the GD2 epitope of the 14g2a-derived scFv is identical between human and mouse. The 14g2a-derived scFv has low affinity binding for GD2 in contrast to another GD2-specific and clinically studied mAb, 3F8.[42] A preclinical murine study suggested possible clinical effects of GD2-specific scFv affinity[36] such as on-target, off-tumor lethal neurotoxicity. In this study, CAR-T-cell infiltration and neuronal destruction was observed in mice administered GD2-CAR-T cells incorporating either a higher affinity mutation in the antigen-binding region of the 14g2a-derived scFv[14] or the 3F8-derived scFv, but not in mice administered GD2-CAR-T cells containing the unmodified 14g2a-derived scFv.[36] Although, in an alternative interpretation of these data, it was posited that excessive cytokine release by the higher affinity GD2-CAR contributed to the neurotoxicity.[43] In a preclinical murine study of DMG in which mice were administered GD2-CAR-T cells containing the unmodified 14g2a-derived scFv, on-target, on-tumor neurotoxicity was observed in the absence of on-target, off-tumor neurotoxicity.[18] These preclinical findings are consistent with earlier extensive testing of GD2-CAR T cells in patients with neuroblastoma[13 17 44] and recent preliminary results in patients with GD2-CAR T-cell-treated DMG in whom tumor-inflammation-associated neurotoxicity without evidence of on-target, off-tumor neurotoxicity was reported.[19]

We have shown levels of GD2 expression in GBM tissues that clearly exceed that detected in adjacent brain confirming the preclinical findings discussed above,[18 36] and an independent pathologist reported no evidence of off-tumor GD2-CAR-T-cell toxicity in the orthotopic GBM xenograft model. Indeed, GD2-CAR-T-treated mice survived significantly longer than their control counterparts. The euthanasia endpoints of poor body condition or excessive weight loss consistent with the GvHD reported by others[18] were reached later than the neurological endpoint, which was reached more often in control mice (figures 3C,D and 5B,C).

The observed lag in the intracranial bioluminescence signal in mice treated with third-generation GD2-CAR-T cells indicated transient tumor control before the tumor escape that preceded onset of clinical signs. However, using another clinically relevant GD2-CAR retrovector encoding the IL-15 transgene, we generated CAR-T cells that resulted in more complete and sustained tumor control. The GD2-CAR-IL-15-T cells further prolonged survival with a 50% complete response rate at 4 weeks post treatment as assessed by bioluminescence intensity. Importantly the GD2-CAR-IL-15 treated group also had significantly lower human GFAP staining in the brain, indicating there was not significant regrowth of GD2-negative $GFAP^+$ tumor (figure 6). This level of control is significant because we use an aggressive patient-derived GBM xenograft that kills within 6 weeks, and we use BLI over an average period of 3 weeks to confirm tumor growth before treatment. In recent publications using different CAR-T products and equivalent aggressive GBM models, similar control has only been achieved by treating at earlier time points (typically days 3–10) or with intracerebral administration.[45–47]

Our results differ from a recent study employing an orthotopic GBM model of xenografts and a second-generation CAR construct based on a novel IgM-derived and human GD2-specific scFv, which the authors report as lacking cross-reactivity with murine GD2. The resulting GD2-CAR-T cells had significant antitumor activity only after intracerebral administration.[24] In contrast, in our study, the GD2-CAR-T cells were active against orthotopic GBM xenografts after intravenous administration, perhaps because of the design of our CAR[48] or of our optimized manufacturing process.[29]Although the intravenous route of administration has usually been adopted in clinical studies of CAR-T-cell therapy in GBM,[7–9] locoregional delivery via intracerebroventricular or intracavitary routes is a promising approach, which has been investigated preclinically,[24 45 49 50] and used on occasion in patients.[10 19]

Immunofluorescence staining and analysis of mouse brains at study endpoints suggested that tumors escaped CAR-T control either because of unrelenting immune selection pressure resulting in antigen loss ($CD3^+$,

residual GD2$^{-/low}$, hGFAP^{+} tumors) or intrinsic CAR-T-cell defects (CD3$^{-/low}$ with residual GD2^{+} tumors) (figure 6 and online supplemental table 2). We hypothesize that the third-generation CAR-T-cell therapy could not kill all antigen-positive tumor cells because of an inadequate initial cell dose, poor tumor infiltration by T cells, or inadequate T-cell functions such as cytotoxicity at the tumor site. The longest surviving mice had the highest levels of CD3^{+} T cells, and the greatest numbers of large intratumoral CD31^{+} blood vessels. This finding raises the possibility that tumor vasculature-normalizing effects of bevacizumab co-treatment may promote T-cell infiltration.[51]

IL-15 co-expression significantly increased GD2-CAR-T-cell engraftment in the spleen and bone marrow of tumor-bearing mice although the improved survival was not simply related to a higher CAR-T-cell dose reaching the tumor. Indeed, GD2-CAR-IL-15-T cells were equivalent to or even less abundant in the brain than third-generation GD2-CAR-T cells. Nonetheless GD2-CAR-IL-15-T cells exerted superior tumor control by measurement of all three tumor markers: GD2, bioluminescence and human GFAP. We hypothesize that the increased effectiveness of the GD2-CAR-IL-15-T cells reflected greater cytotoxic potency or improved survival in the GBM microenvironment or both. Others have reported a distinct phenotype that allows these IL-15-expressing-CAR-T cells to better survive repeated tumor challenge in a neuroblastoma model.[38] Our own RNA sequencing identified multiple differentially expressed pathways associated with chemokine responses and cytotoxicity that were elevated for GD2-CAR-IL-15-T-treated mice.

Other factors that may impair the effectiveness of CAR-T-cell therapy include known tumor microenvironmental inhibitors of T-cell function. The GNS cell line employed in the model showed a range of immune-modulatory molecules (IL-6, programmed death ligand-1, online supplemental figure 10) which may interfere with T-cell function.[52] However, in human GBM xenografts hosted in the brains of NSG mice, and unlike in humans, lymphocytes are absent and microglia and glioma-associated macrophages are relatively lacking, thus indicating that this orthotopic xenograft model does not adequately recapitulate the complex GBM microenvironment in patients. The interaction of the GD2-CAR-T with the myeloid compartment is of particular interest given reported changes to this cell population in clinical trials.[17 19] To fully understand the interplay of CAR-T therapy with the immune microenvironment, syngeneic glioma models are required and would also be important to establish the effects of IL-15 overexpression on immunotoxicity.

Further to our studies of GD2-CAR-T-cell reactivity in orthotopic xenografts of GBM, we assessed the practical aspects of manufacturing CAR-T products for patients with GBM. We identified technical hurdles to autologous CAR-T-cell therapy for patients with GBM including a low yield of lymphocytes and poorer CAR-T expansion, possibly because of oral glucocorticoid therapy, which all patients with GBM received at the time of blood donation for CAR-T-cell manufacturing. Although glucocorticoid usage is often considered as a factor in GBM CAR-T trial design for potential adverse effects on CAR-T effectiveness,[53] it has less frequently been considered for its effects on CAR-T manufacturing. We also noted skewed CD4:CD8 lymphocyte ratios and lower proportions of naïve T cells, which have been reported previously.[33] Nevertheless, potent in vitro functions were observed, and in vivo there was no significant difference in survival between mice treated with healthy-donor derived CAR-T cells or patient with GBM-derived CAR-T cells.

Our advanced planning for a phase 1 trial of GD2-CAR-T-cell therapy in patients with DMG/DIPG (ACTRN12622000675729) has caused us to consider the timing of CAR-T-cell manufacturing and administration with respect to standard treatments. For example, we propose to obtain apheresis products from patients before commencement of palliative radiotherapy, which aims to delay disease progression until the CAR-T-cell product is ready for administration. Moreover, given the key role of blood vessels in T-cell infiltration of tumors we also propose to use the anti-Vascular Endothelial Growth Factor (VEGF)-neutralizing mAb, bevacizumab, in combination with GD2-CAR-T-cell therapy to mitigate brain swelling from CAR-T cell-related neuroinflammation and potentially to stabilize the tumor vasculature so that T-cell access to the tumor is promoted.[54–56]

In summary, by using primary patient samples for manufacturing and disease modeling in this preclinical study, we have identified several factors associated with the duration of tumor control and ultimately the survival of GBM-bearing mice. Successful CAR-T-cell engraftment in bone marrow, high absolute numbers of tumor-infiltrating CAR-T cells and the development of a T-cell-supportive intratumoral vasculature were all associated with improved survival following treatment with third-generation GD2-CAR-T cells that will be used in our upcoming phase 1 trials. Treatment with GD2-CAR-T cells enhanced with an IL-15 transgene had improved engraftment and significantly better tumor control, and without an evident increase in the number of tumor-infiltrating CAR-T cells. Our results support the case for further toxicity studies that may best be undertaken in orthotopic syngraft models of GBM in immunocompetent mice. In considering clinical investigation of this approach in GBM, the incorporation of a suicide gene may mitigate potential risks related to CAR-T cells carrying an IL-15 transgene including autonomous proliferation[39] and neurotoxicity.[57]

MATERIALS AND METHODS

Detailed methodology provided in online supplemental methods.

Human tumor material

Tumor tissue and blood from patient with GBM were obtained through the SANTB. Fresh tissue samples were prepared as described previously.[27] All human specimens were used in accordance with the Declaration of Helsinki, and participants provided written consent.

Culture of GNS tumor cell lines and CAR-T cells

GNS cells were cultured in StemPro NSC medium (Thermo Fisher) as described previously.[27] The neuroblastoma line LAN-1 was maintained in Dubesco's Modified Eagle Medium (DMEM)-F12 media with 10% Fetal Calf Serum, 1% Glutamax, 1% Pen/Step. Peripheral T cells were separated from blood samples and used to generate GD2-specific third-generation CAR-T cells using GD2-iCAR retroviral vector SFG.iCasp9.2A.14g2a.CD28.OX40.zeta supernatant (Center for Cell and Gene Therapy, Baylor College of Medicine, Houston, Texas, USA) and our clinical manufacturing protocol as described previously.[29] The second-generation GD2-CAR-IL-15 retrovector[38 58 59] was obtained under a material transfer agreement with Baylor College of Medicine with the kind assistance of Professor Leonid Metelitsa. Post-thawing, CAR-T-cell products were maintained in TEXMACS media (Miltenyi) with 10 ng/mL IL-7 and 5 ng/mL IL-15 for a maximum of 10 days.

Immunofluorescence staining of cryosections

Sections were cut from Optimal Cutting Temperature (OCT) compound-embedded human GBM, human adjacent normal brain, and mouse brain tissues (5–6 µm thickness).

Tissue sections were stained using 5 µg/mL purified mouse anti-human CD3 (UCHT1; BioLegend) and 4 µg/mL purified hamster anti-mouse CD31 (2H8; Thermo Fisher Scientific) with goat anti-mouse IgG AF647 (Thermo Fisher Scientific) and goat anti-hamster IgG AF488 (Abcam) detection antibodies, and mouse anti-GD2-FITC (14.G2A; BD) at a dilution of 1:100. GFAP was detected with polyclonal rabbit-anti human GFAP (1:500, Agilent) and donkey anti-rabbit IgG AF55 detection (1:500, Thermo Fisher Scientific).

Whole-slide imaging was performed on a Zeiss Axio Scan.Z1 slide-scanner using 20× objective and ZEN 3.1 Blue system software. Fluorescence overlays were created by merging channels and applying false color using FIJI (ImageJ, National Institutes of Health).

For further detail see online supplemental methods.

Flow cytometry

Stained cells were analyzed on a BD LSR Fortessa (BD Biosciences) or a BD FACSymphony A5 (BD Biosciences) with FlowJo Software V. 10.8.1 (BD Biosciences). For further detail see online supplemental methods.

Orthotopic xenograft model

Animal experiments were conducted under a protocol approved by the University of South Australia Animal Ethics Committee (#U44-19). A Stoelting motorized stereotactic alignment and injection unit was used to deliver 2 µL of patient-derived GNS cells ($2–5\times10^5$ cells) over 4 min, 3 mm deep into the right hemisphere of 6–8 weeks old female NOD-SCID-gamma-null (NSG) mice (Animal Resources Centre, Perth). Mice received daily clinical checks and weekly BLI to monitor tumor growth. BLI was performed using an IVIS Lumina S5 after intraperitoneal injection of 100 µL of 30 mg/mL luciferin in saline.

CAR-T-cell treatment (up to 1×10^7 total T cells; $1.5–4\times10^6$ CAR^+ T cells) was administered intravenously *via* tail-vein injection once tumor growth had been observed for two consecutive weeks, confirming tumor engraftment at days 17–28 in these experiments. Mice were reassigned to treatment cages so that the average luminescence for each cage was equivalent. Mice that failed to show tumor growth at day 28 were excluded from the experiment. Sample sizes were based on power calculations to detect 50% or greater reduction in tumor volume with 95% confidence, and 50% or greater increase in T-cell infiltration in the brain. Defined humane endpoints for euthanasia included loss of >15% body weight from starting weight, a body condition score of <2 (underconditioned,[60] and neurological signs including head-tilt, loss of balance and circling movement.

Statistics

Data were analyzed using GraphPad Prism V.9.3.1. Single-variable data were analyzed by one-way analysis of variance (ANOVA), two-variable date were analyzed by two-way ANOVA and Tukey's multiple comparison post-tests. Multiple survival curves were analyzed using the logrank test for trend, and specific comparisons of two selected curves employed the Gehan-Breslow-Wilcoxon test. Statistical significance is represented on graphs as * ≤0.05, ** ≤0.01 and *** ≤0.001.

Author affiliations
[1]Translational Oncology Laboratory, Centre for Cancer Biology, SA Pathology and Univeristy of South Australia, Adelaide, South Australia, Australia
[2]Cancer Clinical Trials Unit, Royal Adelaide Hospital, Adelaide, South Australia, Australia
[3]Adelaide Medical School, The University of Adelaide, Adelaide, South Australia, Australia
[4]Molecular Therapeutics Laboratory, Centre for Cancer Biology, Adelaide, South Australia, Australia
[5]Flinders Health and Medical Research Institute, Flinders University, Adelaide, South Australia, Australia
[6]Department of Neurosurgery, Flinders Medical Centre, Bedford Park, South Australia, Australia
[7]Children's Cancer Institute, Lowy Cancer Research Centre, Sydney, New South Wales, Australia
[8]School of Women's and Children's Health, University of New South Wales, Sydney, New South Wales, Australia
[9]Kid's Cancer Centre, Sydney Children's Hospital, Randwick, NSW, Australia

Acknowledgements We acknowledge Professor Malcolm Brenner, Professor Gianpietro Dotti, and Assistant Professor Eric Yvon for provision of the original third-generation GD2-specific CAR-T cell retroviral vector. We acknowledge Professor Leonid Metelitsa and Professor Gianpietro Dotti for provision of the second-generation GD2-specific and IL-15 producing CAR retroviral vector and Professor Bryan Day for GNS lines. We thank Bryan Gardam for his analysis of macrophage

and microglia in NSG mice. We acknowledge Steven Roberts and Dr Andrew Lim (BD Biosciences) for technical advice in designing multicolor flow panels for use on the BD FACS Symphony and Dr Agatha Labrinidis for technical microscopy support. We thank Guillermo Gomez for provision of the human GFAP antibody. We acknowledge Miltenyi Biotec for support in obtaining the Clinimacs Plus instrument used in our clinical manufacturing, and Paula Stoddart for technical advice. We thank the Zero Childhood Cancer Initiative for access to archival DIPG patient material, and the KOALA clinical trials team (Emma McCormack, Lily Wong, Alison Rego) for recruitment of patients with diffuse intrinsic pontine glioma to give fresh blood samples. We also acknowledge the support and generosity of the patients and medical and technical staff from SA Pathology and the SA Neurological Tumor Bank (supported by Flinders University, Flinders Foundation and The NeuroSurgical Research Foundation), who made collection of tissue specimens possible. We thank clinical pathologists at SA Pathology and veterinary pathologists at Gribbles pathology (Adelaide) for their histopathologic evaluations. RNA-sequencing experiments were performed at the Australian Cancer Research Foundation (ACRF) Cancer Genomics and Cancer Discovery Accelerator facilities at SA Pathology, established with the generous support of the Australian Cancer Research Foundation, and bioinformatics support was kindly provided by John Toubia.

Contributors TG: Conceptualization, investigation, formal analysis, methodology, data curation, writing—original draft, writing—review and editing, funding acquisition, and is guarantor for the content. LME: Conceptualization, investigation, data curation, funding acquisition, methodology, resources, supervision, writing—review and editing. NTHT: Investigation, formal analysis, methodology, data curation. PMK: Investigation, formal analysis, methodology, visualization. KS: Investigation, formal analysis. WY: Investigation, methodology. ECFY: Investigation. NLW: Investigation. BLG: Investigation, methodology. MNT: Investigation, methodology. RO: Resources, data curation. SP: Resources, data curation. JN: Resources, data curation. OV: Resources. DSZ: Resources, data curation. SMP: Funding acquisition, resources. MPB: Conceptualization, funding acquisition, resources, supervision, writing—review and editing.

Funding This work was supported by the NeuroSurgical Research Foundation, The Hospital Research Foundation Group, the Cancer Council SA Beat Cancer Project (Hospital Research Package and Fellowship to TG), Cancer Australia, the Health Services Charitable Gifts Board (Adelaide), Tour de Cure, the Ray & Shirl Norman Cancer Research Trust, the Mark Hughes Foundation, the National Health and Medical Research Council (Fellowship to SMP), and the Fay Fuller Foundation (Fellowship to MNT).

Competing interests None declared.

Patient consent for publication Not applicable.

Ethics approval Use of patient with human glioblastoma samples was approved by the Central Adelaide Local Health Network Human Research Ethics Committee (CALHN HREC; approval number R20160727; R20170821). Patient with melanoma blood samples for CAR-T manufacturing were obtained under the CARPETS trial protocol (CALHN HREC; approval number R20100524). Samples from patients with diffuse intrinsic pontine glioma were obtained from the Zero Childhood Cancer Initiative (approval number ZCC039), and from the Sydney Children's Hospital (SCHN HREC; approval 2019/ETH05438). Participants gave informed consent to participate in the study before taking part.

Provenance and peer review Not commissioned; externally peer reviewed.

Data availability statement Data are available upon reasonable request. Original data sets (de-identified patient data, scanned microscopy images, flow cytometry FCS files, mouse imaging files, raw impedance values for cytotoxicity assays, mouse clinical records) will be made available by the authors upon reasonable request to the corresponding author (Dr Tessa Gargett, Royal Adelaide Hospital, Adelaide, SA 5000, E: tessa.gargett@sa.gov.au).

ORCID iDs
Tessa Gargett http://orcid.org/0000-0003-3713-1373
Lisa M Ebert http://orcid.org/0000-0002-8041-9666
Michael P Brown http://orcid.org/0000-0002-5796-1932

REFERENCES

1 Poon MTC, Sudlow CLM, Figueroa JD, *et al*. Longer-term (≥2 years) survival in patients with glioblastoma in population-based studies pre- and post-2005: a systematic review and meta-analysis. *Sci Rep* 2020;10:11622.
2 Vitanza NA, Monje M. Diffuse intrinsic pontine glioma: from diagnosis to next-generation clinical trials. *Curr Treat Options Neurol* 2019;21:37.
3 Muftuoglu Y, Liau LM. Results from the CheckMate 143 clinical trial: stalemate or new game strategy for glioblastoma immunotherapy? *JAMA Oncol* 2020;6:987–9.
4 Porter DL, Hwang W-T, Frey NV, *et al*. Chimeric antigen receptor T cells persist and induce sustained remissions in relapsed refractory chronic lymphocytic leukemia. *Sci Transl Med* 2015;7:ra139.
5 Maude SL, Laetsch TW, Buechner J, *et al*. Tisagenlecleucel in children and young adults with B-cell lymphoblastic leukemia. *N Engl J Med Overseas Ed* 2018;378:439–48.
6 Sadelain M, Rivière I, Riddell S. Therapeutic T cell engineering. *Nature* 2017;545:423–31.
7 Goff SL, Morgan RA, Yang JC, *et al*. Pilot trial of adoptive transfer of chimeric antigen Receptor–transduced T cells targeting EGFRvIII in patients with glioblastoma. *J Immunother* 2019;42:126–35.
8 Ahmed N, Brawley V, Hegde M, *et al*. Her2-Specific chimeric antigen receptor-modified virus-specific T cells for progressive glioblastoma: a phase 1 dose-escalation trial. *JAMA Oncol* 2017;3:1094–101.
9 O'Rourke DM, Nasrallah MP, Desai A, *et al*. A single dose of peripherally infused EGFRvIII-directed CAR T cells mediates antigen loss and induces adaptive resistance in patients with recurrent glioblastoma. *Sci Transl Med* 2017;9:eaaa0984.
10 Brown CE, Alizadeh D, Starr R, *et al*. Regression of glioblastoma after chimeric antigen receptor T-cell therapy. *N Engl J Med Overseas Ed* 2016;375:2561–9.
11 Brown MP, Ebert LM, Gargett T. Clinical chimeric antigen receptor-T cell therapy: a new and promising treatment modality for glioblastoma. *Clin Transl Immunology* 2019;8:e1050.
12 Suzuki M, Cheung N-KV. Disialoganglioside GD2 as a therapeutic target for human diseases. *Expert Opin Ther Targets* 2015;19:349–62.
13 Pule MA, Savoldo B, Myers GD, *et al*. Virus-Specific T cells engineered to coexpress tumor-specific receptors: persistence and antitumor activity in individuals with neuroblastoma. *Nat Med* 2008;14:1264–70.
14 Horwacik I, Golik P, Grudnik P, *et al*. Structural basis of GD2 ganglioside and mimetic peptide recognition by 14G2a antibody. *Mol Cell Proteomics* 2015;14:2577–90.
15 Yu AL, Gilman AL, Ozkaynak MF, *et al*. Anti-Gd2 antibody with GM-CSF, interleukin-2, and isotretinoin for neuroblastoma. *N Engl J Med* 2010;363:1324–34.
16 Gargett T, Yu W, Dotti G, *et al*. GD2-specific CAR T cells undergo potent activation and deletion following antigen encounter but can be protected from activation-induced cell death by PD-1 blockade. *Mol Ther* 2016;24:1135–49.
17 Heczey A, Louis CU, Savoldo B, *et al*. Car T cells administered in combination with Lymphodepletion and PD-1 inhibition to patients with neuroblastoma. *Molecular Therapy* 2017;25:2214–24.
18 Mount CW, Majzner RG, Sundaresh S, *et al*. Potent antitumor efficacy of anti-GD2 CAR T cells in H3-K27M^{+} diffuse midline gliomas. *Nat Med* 2018;24:572–9.
19 Majzner RG, Ramakrishna S, Yeom KW, *et al*. GD2-CAR T cell therapy for H3K27M-mutated diffuse midline gliomas. *Nature* 2022;603:934–41.
20 Marx S, Wilken F, Wagner I, *et al*. Gd2 targeting by dinutuximab beta is a promising immunotherapeutic approach against malignant glioma. *J Neurooncol* 2020;147:577–85.
21 Fleurence J, Bahri M, Fougeray S, *et al*. Impairing temozolomide resistance driven by glioma stem-like cells with adjuvant immunotherapy targeting O-acetyl GD2 ganglioside. *Int J Cancer* 2020;146:424–38.
22 Golinelli G, Grisendi G, Prapa M, *et al*. Targeting GD2-positive glioblastoma by chimeric antigen receptor empowered mesenchymal progenitors. *Cancer Gene Ther* 2020;27:558–70.

23 Murty S, Haile ST, Beinat C, *et al*. Intravital imaging reveals synergistic effect of car T-cells and radiation therapy in a preclinical immunocompetent glioblastoma model. *Oncoimmunology* 2020;9:1757360.
24 Prapa M, Chiavelli C, Golinelli G, *et al*. Gd2 CAR T cells against human glioblastoma. *NPJ Precis Oncol* 2021;5:93.
25 Wikstrand CJ, Fredman P, Svennerholm L, *et al*. Detection of glioma-associated gangliosides GM2, GD2, GD3, 3'-isoLM1 3',6'-isoLD1 in central nervous system tumors in vitro and in vivo using epitope-defined monoclonal antibodies. *Prog Brain Res* 1994;101:213–23.
26 Mennel HD, Bosslet K, Geissel H, *et al*. Immunohistochemically visualized localisation of gangliosides Glac2 (GD3) and Gtri2 (GD2) in cells of human intracranial tumors. *Exp Toxicol Pathol* 2000;52:277–85.
27 Ebert LM, Yu W, Gargett T, *et al*. Endothelial, pericyte and tumor cell expression in glioblastoma identifies fibroblast activation protein (FAP) as an excellent target for immunotherapy. *Clin Transl Immunology* 2020;9:e1191.
28 Sorokin M, Kholodenko I, Kalinovsky D, *et al*. Rna sequencing-based identification of ganglioside GD2-positive cancer phenotype. *Biomedicines*2020;8:142.
29 Gargett T, Truong NGA, Ebert LM, *et al*. Optimization of manufacturing conditions for chimeric antigen receptor T cells to favor cells with a central memory phenotype. *Cytotherapy* 2019;21:593–602.
30 Huang Z, Wu L, Hou Z, *et al*. Eosinophils and other peripheral blood biomarkers in glioma grading: a preliminary study. *BMC Neurol* 2019;19:313.
31 Vaios EJ, Winter SF, Muzikansky A, *et al*. Eosinophil and lymphocyte counts predict bevacizumab response and survival in recurrent glioblastoma. *Neurooncol Adv* 2020;2:vdaa031.
32 Madhugiri VS, Moiyadi AV, Shetty P, *et al*. Analysis of factors associated with long-term survival in patients with glioblastoma. *World Neurosurg* 2021;149:e758–65.
33 Chongsathidkiet P, Jackson C, Koyama S, *et al*. Sequestration of T cells in bone marrow in the setting of glioblastoma and other intracranial tumors. *Nat Med* 2018;24:1459–68.
34 Gargett T, Brown MP. Different cytokine and stimulation conditions influence the expansion and immune phenotype of third-generation chimeric antigen receptor T cells specific for tumor antigen GD2. *Cytotherapy* 2015;17:487–95.
35 Davenport AJ, Jenkins MR, Cross RS, *et al*. Car-T cells Inflict sequential killing of multiple tumor target cells. *Cancer Immunol Res* 2015;3:483–94.
36 Richman SA, Nunez-Cruz S, Moghimi B, *et al*. High-Affinity GD2-Specific CAR T cells induce fatal encephalitis in a preclinical neuroblastoma model. *Cancer Immunol Res* 2018;6:36–46.
37 Gargett T, Fraser CK, Dotti G, *et al*. Braf and MEK inhibition variably affect GD2-specific chimeric antigen receptor (CAR) T-cell function in vitro. *J Immunother* 2015;38:12–23.
38 Chen Y, Sun C, Landoni E, *et al*. Eradication of neuroblastoma by T cells redirected with an optimized GD2-Specific chimeric antigen receptor and interleukin-15. *Clin Cancer Res* 2019;25:2915–24.
39 Reppel L, Tsahouridis O, Akulian J, *et al*. Targeting disialoganglioside GD2 with chimeric antigen receptor-redirected T cells in lung cancer. *J Immunother Cancer* 2022;10:e003897.
40 Rafiq S, Hackett CS, Brentjens RJ. Engineering strategies to overcome the current roadblocks in car T cell therapy. *Nat Rev Clin Oncol* 2020;17:147–67.
41 Kollis PM, Ebert LM, Toubia J, *et al*. Characterising distinct migratory profiles of infiltrating T-cell subsets in human glioblastoma. *Front Immunol* 2022;13:850226.
42 Cheung N-KV, Guo H, Hu J, *et al*. Humanizing murine IgG3 anti-GD2 antibody m3F8 substantially improves antibody-dependent cell-mediated cytotoxicity while retaining targeting in vivo. *Oncoimmunology* 2012;1:477–86.
43 Majzner RG, Weber EW, Lynn RC, *et al*. Neurotoxicity associated with a high-affinity GD2 CAR-Letter. *Cancer Immunol Res* 2018;6:494–5.
44 Straathof K, Flutter B, Wallace R, *et al*. Antitumor activity without on-target off-tumor toxicity of GD2-chimeric antigen receptor T cells in patients with neuroblastoma. *Sci Transl Med* 2020;12:eabd6169.
45 Rousso-Noori L, Mastandrea I, Talmor S, *et al*. P32-specific CAR T cells with dual antitumor and antiangiogenic therapeutic potential in gliomas. *Nat Commun* 2021;12:3615.
46 Xu C, Bai Y, An Z, *et al*. IL-13Rα2 humanized scFv-based CAR-T cells exhibit therapeutic activity against glioblastoma. *Mol Ther Oncolytics* 2022;24:443–51.
47 an Z, Hu Y, Bai Y, *et al*. Antitumor activity of the third generation EphA2 CAR-T cells against glioblastoma is associated with interferon gamma induced PD-L1. *Oncoimmunology* 2021;10:1960728.
48 Pulè MA, Straathof KC, Dotti G, *et al*. A chimeric T cell antigen receptor that augments cytokine release and supports clonal expansion of primary human T cells. *Mol Ther* 2005;12:933–41.
49 Donovan LK, Delaidelli A, Joseph SK, *et al*. Locoregional delivery of CAR T cells to the cerebrospinal fluid for treatment of metastatic medulloblastoma and ependymoma. *Nat Med* 2020;26:720–31.
50 Priceman SJ, Tilakawardane D, Jeang B, *et al*. Regional Delivery of Chimeric Antigen Receptor-Engineered T Cells Effectively Targets $HER2^+$ Breast Cancer Metastasis to the Brain. *Clin Cancer Res* 2018;24:95–105.
51 Bocca P, Di Carlo E, Caruana I, *et al*. Bevacizumab-mediated tumor vasculature remodelling improves tumor infiltration and antitumor efficacy of GD2-CAR T cells in a human neuroblastoma preclinical model. *Oncoimmunology* 2018;7:e1378843.
52 Tsukamoto H, Fujieda K, Senju S, *et al*. Immune-Suppressive effects of interleukin-6 on T-cell-mediated anti-tumor immunity. *Cancer Sci* 2018;109:523–30.
53 Brudno JN, Kochenderfer JN. Toxicities of chimeric antigen receptor T cells: recognition and management. *Blood* 2016;127:3321–30.
54 Hodi FS, Lawrence D, Lezcano C, *et al*. Bevacizumab plus ipilimumab in patients with metastatic melanoma. *Cancer Immunol Res* 2014;2:632–42.
55 Tamura R, Tanaka T, Ohara K, *et al*. Persistent restoration to the immunosupportive tumor microenvironment in glioblastoma by bevacizumab. *Cancer Sci* 2019;110:499–508.
56 Li Shu-Jin, Chen Jia-Xian, Sun Zhi-Jun. Improving antitumor immunity using antiangiogenic agents: mechanistic insights, current progress, and clinical challenges. *Cancer Commun* 2021;41:830–50.
57 Gofshteyn JS, Shaw PA, Teachey DT, *et al*. Neurotoxicity after CTL019 in a pediatric and young adult cohort. *Ann Neurol* 2018;84:537–46.
58 Xu X, Huang W, Heczey A, *et al*. NKT Cells Coexpressing a GD2-Specific Chimeric Antigen Receptor and IL15 Show Enhanced *In Vivo* Persistence and Antitumor Activity against Neuroblastoma. *Clin Cancer Res* 2019;25:7126–38.
59 Heczey A, Courtney AN, Montalbano A, *et al*. Anti-Gd2 CAR-NKT cells in patients with relapsed or refractory neuroblastoma: an interim analysis. *Nat Med* 2020;26:1686–90.
60 Ullman-Culleré MH, Foltz CJ. Body condition scoring: a rapid and accurate method for assessing health status in mice. *Lab Anim Sci* 1999;49:319–23.